

Thrombospondins Are Astrocyte-Secreted Proteins that Promote CNS Synaptogenesis

Karen S. Christopherson,^{1,6,*} Erik M. Ullian,^{6,7}
Caleb C.A. Stokes,¹ Christine E. Mullowney,¹
Johannes W. Hell,² Azin Agah,³ Jack Lawler,⁴
Deane F. Mosher,⁵ Paul Bornstein,³
and Ben A. Barres¹

¹Department of Neurobiology
Stanford University School of Medicine
Stanford, California 94305

²Department of Pharmacology
University of Iowa
Iowa City, Iowa 52242

³Departments of Biochemistry and Medicine
University of Washington
Seattle, Washington 98195

⁴Department of Pathology
Beth Israel Deaconess Medical Center and Harvard
Medical School
Boston, Massachusetts 02115

⁵Department of Medicine
Medical Sciences Center
University of Wisconsin
Madison, Wisconsin 53706

Summary

The establishment of neural circuitry requires vast numbers of synapses to be generated during a specific window of brain development, but it is not known why the developing mammalian brain has a much greater capacity to generate new synapses than the adult brain. Here we report that immature but not mature astrocytes express thrombospondins (TSPs)-1 and -2 and that these TSPs promote CNS synaptogenesis *in vitro* and *in vivo*. TSPs induce ultrastructurally normal synapses that are presynaptically active but postsynaptically silent and work in concert with other, as yet unidentified, astrocyte-derived signals to produce functional synapses. These studies identify TSPs as CNS synaptogenic proteins, provide evidence that astrocytes are important contributors to synaptogenesis within the developing CNS, and suggest that TSP-1 and -2 act as a permissive switch that times CNS synaptogenesis by enabling neuronal molecules to assemble into synapses within a specific window of CNS development.

Introduction

Is synaptogenesis controlled solely by the pre- and postsynaptic neurons, or are there pivotal nonneuronal determinants that help to control the timing, location, and number of synapses that form? We have been investigating the role of astrocytes, which ensheath the syn-

apses throughout the CNS, in controlling synaptogenesis. In previous studies, we found that, when purified rat retinal ganglion cells (RGCs) are cultured in defined serum-free conditions that fully support their survival and growth, they form few synapses unless cultured with astrocytes, as measured by electrophysiology, FM1-43 imaging, immunostaining, and electron microscopy (Mauch et al., 2001; Nagler et al., 2001; Pfrieger and Barres, 1997; Ullian et al., 2004a). Similarly, purified spinal motor neurons form few synapses unless cultured with Schwann cells or astrocytes (Ullian et al., 2004c). Culturing RGCs under feeding layers of astrocytes, without direct contact, is sufficient to enhance synapse number, indicating that these effects are mediated by one or more soluble signals secreted by astrocytes (Nagler et al., 2001; Pfrieger and Barres, 1997; Ullian et al., 2001). The astrocyte-induced increase in synapse number is not due to the absence of the normal target of these neurons because the same increase in RGC synapse number and function is induced between RGCs and their normal target neurons purified from the superior colliculus (Ullian et al., 2001).

What is the identity of these astrocyte-secreted signals? Here we identify thrombospondin family members (TSPs) as necessary and sufficient synaptogenic components of astrocyte-conditioned medium (ACM). TSPs are large oligomeric extracellular matrix proteins that mediate cell-cell and cell-matrix interactions by binding an array of membrane receptors, other extracellular matrix proteins, and cytokines (Adams, 2001; Adams and Tucker, 2000; Bornstein, 2001; Lawler, 2000). There are five TSPs, each encoded by a separate gene. Although several TSPs are expressed in the brain, the functions of these TSPs are unknown (Adams and Tucker, 2000; Iruela-Arispe et al., 1993; Scott-Drew and French-Constant, 1997). TSP1 and TSP2 are closely related trimeric proteins that share the same set of structural and functional domains. TSP4, which is pentameric and has a different domain structure from TSP1 and TSP2, is present in the adult nervous system where it is localized to some CNS synapses as well as the neuromuscular junction (Arber and Caroni, 1995). The findings we report here identify TSPs as astrocyte-secreted proteins that promote the formation of ultrastructurally normal CNS synapses and reveal that additional, as yet unidentified, astrocyte-derived signals control postsynaptic function.

Results

Astrocytes Secrete Two Activities that Affect Synapse Formation and Function Differentially

In order to establish an assay for biochemical studies to identify synaptogenic activities secreted by astrocytes, we compared the ability of astrocyte-conditioned medium (ACM) and astrocyte feeding layers ("Astros") to induce synapses on RGCs (Figure 1A). Synapses were detected as yellow puncta, representing colocalization of immunoreactivity to the pre- and

*Correspondence: ksc@stanford.edu

⁶These authors contributed equally to this work.

⁷Present address: Departments of Ophthalmology and Physiology, University of California, San Francisco, California, 94143, USA

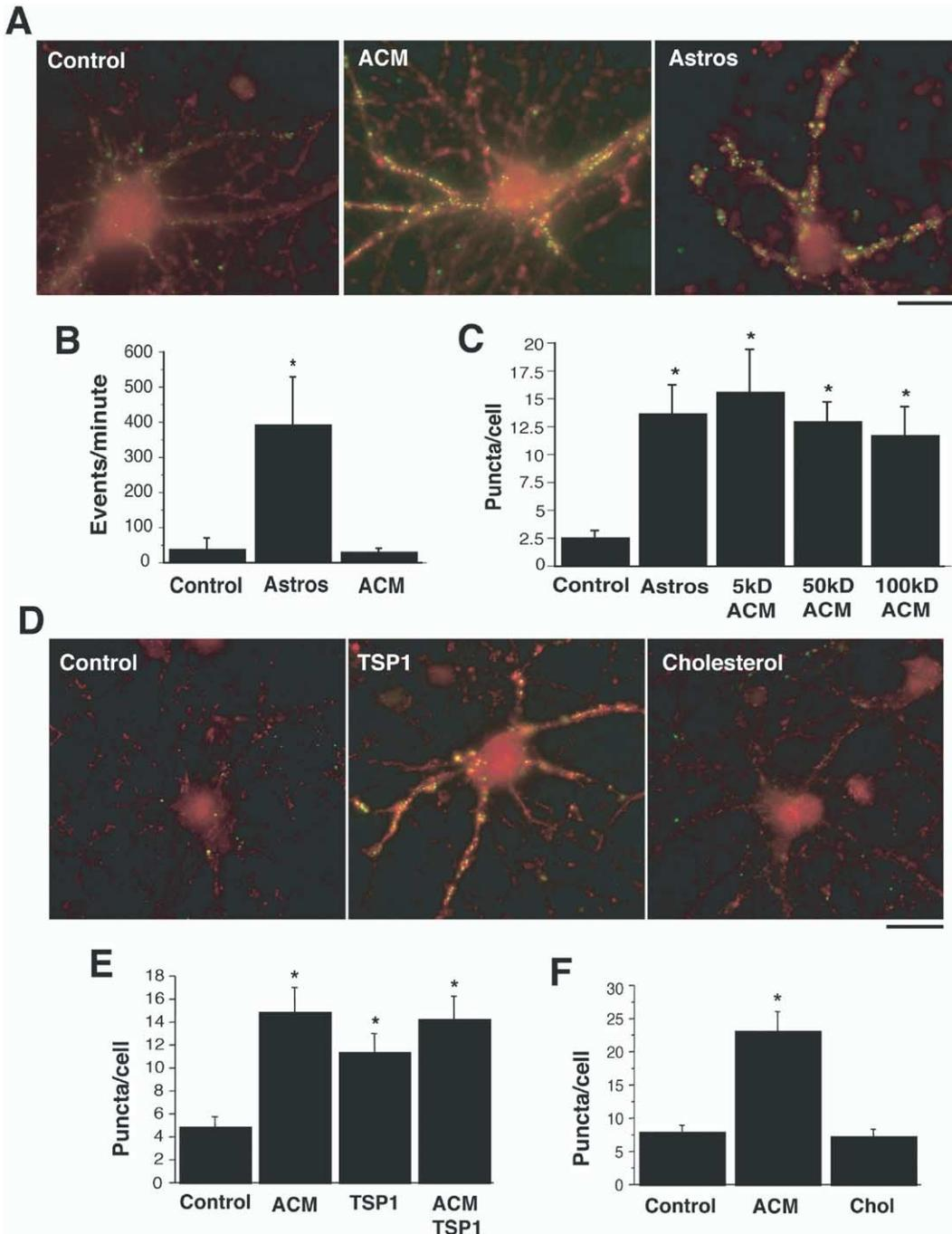


Figure 1. TSP1 Mimics the Synapse-Promoting Activity of ACM

(A) Immunostaining of RGCs for colocalization of presynaptic synaptotagmin (red) and postsynaptic PSD-95 (green) shows few synaptic puncta in the absence of astrocytes (Control) but many in the presence of astrocyte-conditioned medium (ACM) or a feeding layer of astrocytes (Astros), indicating that astrocytes secrete a synapse-promoting activity that is also active in ACM.

(B) Astrocyte feeding layer (Astros) increases frequency of spontaneous mEPSCs above control, while ACM does not.

(C) Synapse-promoting activity in ACM is over 100 kDa. ACM was concentrated with molecular weight cutoff (MWCO) filters of 5, 50, and 100 kDa. The number of puncta from ACM prepared with a 100 kDa MWCO filter is similar to the number of puncta produced by astrocyte feeding layer, indicating that the astrocyte-derived synapse-promoting activity is over 100 kDa.

(D) Immunostaining for colocalization of presynaptic synaptotagmin (red) and postsynaptic PSD-95 (green) shows few RGC synaptic puncta in the absence of astrocytes (Control) but many in the presence of 5 μ g/ml thrombospondin 1 (TSP1), indicating that TSP1 is sufficient to increase synaptic puncta on neurons. Cholesterol induces no increase in puncta.

(E) Quantification of the effects of ACM, TSP1, and ACM + TSP1 on synaptic puncta. ACM and TSP1 significantly increase the number of synaptic puncta over control. ACM + TSP1 increases synaptic puncta to the same extent as either ACM or TSP1 alone, indicating that the effect of ACM is not additive with the effect of TSP1.

(F) Cholesterol (10 μ g/ml) does not increase the number of synaptic puncta in neurons. Asterisks in all panels correspond to $p < 0.05$ compared to control. Error bars are the mean \pm SEM. Scale bars are 30 μ m.

postsynaptic markers synaptotagmin and PSD-95, respectively. Each yellow punctum corresponds to the site of a single functional synapse (Ullian et al., 2001). As previously described (Ullian et al., 2001), RGCs cultured for several days below a feeding layer of astrocytes have 7-fold more functional synapses than RGCs cultured alone, as assayed by whole-cell patch recording (Figure 1B). When RGCs were cultured in ACM, there was an increase in the number of structural synapses, indicated by an increase in both the number and colocalization of pre- and postsynaptic puncta in the presence of ACM (Figure 1A); however, these synapses were not functional, as indicated by the frequency of synaptic currents (Figure 1B). Despite this lack of function, quantification of immunostaining showed that ACM induced as many structural synapses as an astrocyte feeding layer (Figure 1C). This suggests that there are at least two signals secreted by astrocytes: one that is present in ACM that increases the number of structural synapses and a second signal either not produced in the absence of RGCs or lost during preparation of ACM (data not shown) that induces functionality.

TSP1 Is Sufficient to Mimic the ACM-Induced Increase in Synapse Number

Having established an assay in which ACM exhibits the same ability to induce synaptic puncta as an astrocyte feeding layer, we next investigated the molecular weight of the synaptogenic ACM component. We found that all of the synapse-promoting activity in ACM was larger than 100 kDa (Figure 1C), and the majority of the activity was still retained with a 300 kDa cutoff filter (data not shown). To test whether ApoE-containing particles could be responsible for the activity as previously reported (Mauch et al., 2001), we immunodepleted ApoE-containing complexes from ACM. Despite depletion of virtually all of the ApoE protein, ACM induced the same number of synapses (see Supplemental Figure S1 in the Supplemental Data available with this article online). In addition, we found that treatment of RGCs with either ApoE (data not shown) or cholesterol (Figures 1D and 1F) had no effect on synapse number. Therefore, ApoE bound cholesterol is not responsible for the synapse-promoting activity of ACM. However, cholesterol does strongly enhance synaptic efficacy, as previously reported (Mauch et al., 2001; Supplemental Figure S1).

The large size of the synaptogenic ACM activity, together with our unpublished observation that the activity is heparin binding (data not shown), strongly suggested the possibility that the activity is an extracellular matrix protein. We investigated the possibility that TSPs contribute to the synaptogenic activity of ACM because TSPs form large >500 kDa oligomeric complexes, are made by astrocytes *in vitro* and *in vivo* (Adams and Tucker, 2000; Iruela-Arispe et al., 1993; Scott-Drew and French-Constant, 1997), and are well established as regulators of cell attachment in nonneural cells, and at least one family member is localized to the neuromuscular junction and to some synapses within the CNS (Arber and Caroni, 1995). Purified TSP1 from human platelets increased the number of synaptic puncta in RGCs to a

similar degree as ACM (Figures 1D and 1E). The number of puncta per RGC induced by TSP1 increased in a dose-dependent manner with concentrations of TSP1 ranging from 2 to 20 nM; 10 nM was the plateau concentration and was used in all subsequent experiments (data not shown). We found no difference in the average radii or the distance between the centers of colocalized puncta between conditions (Supplemental Table S1), indicating that the increase in synapse number was not simply due to an increase in the size of the few synaptic puncta present in control conditions. TSP1-induced synaptic puncta exhibited immunoreactivity for a large variety of presynaptic proteins including synaptotagmin, synapsin, and Bassoon as well as postsynaptic proteins including PSD-95, SAP102, and Homer (Supplemental Figure S6). To determine whether the increase in synapse number by TSP1 involved increased levels of synaptic proteins, we measured protein levels in control RGCs and RGCs treated with TSP1. Similar to our previous results with astrocytes (Ullian et al., 2001), we found that RGCs treated with TSP1 did not have significantly increased levels of synaptic proteins compared to control cultures (Supplemental Figure S2), indicating that TSP is affecting synaptic protein localization. In addition, the increase in synapses seen with TSP1 treatment was not due to an increase in axon length (DeFreitas et al. [1995], Neugebauer et al. [1991]; axon length 1 day in culture control, $196 \pm 15 \mu\text{m}$; TSP1, $223 \pm 18 \mu\text{m}$; means \pm SD, $n = 30$; $p > 0.05$), dendrite length, or altered process morphology (Supplemental Figure S3).

To determine whether the synaptogenic effect was specific to TSP1, we tested a panel of extracellular matrix molecules known to be secreted by astrocytes (including fibronectin, vitronectin, tenascin C, osteonectin/SPARC, osteopontin, chondroitin sulfate proteoglycans A and C, biglycan, decorin, and agrin) as well as battery of peptide trophic factors (including $\text{TNF}\alpha$, IL-6, GDNF, bFGF, TGF β 1, HGF, and pleiotrophin). None of these molecules had a significant effect on synapse number (Supplemental Figure S3). In addition, BDNF, CNTF, and insulin are present in our medium even in control conditions where few synapses form.

ACM and TSP1-Induced Synapses Are Ultrastructurally Normal

Are the ACM- and TSP1-induced synapses ultrastructurally normal? We used electron microscopy to study ACM- and TSP1-induced synapses in fine detail. Synapses induced by TSP1 and ACM were ultrastructurally identical to the electrophysiologically active synapses induced by a feeding layer of astrocytes. Pre- and postsynaptic specializations could be easily detected in RGCs cultured under both conditions as well as with an astrocyte feeding layer (Figure 2A). There was no difference in the length or thickness of the postsynaptic density (PSD) between synapses induced by TSP1 or an astrocyte feeding layer (PSD length, $380 \pm 197 \text{ nm}$ [TSP] versus $398 \pm 209 \text{ nm}$ [Astro, $p = 0.8$]; PSD thickness, $46 \pm 5 \text{ nm}$ [TSP] versus $50 \pm 8 \text{ nm}$ [Astro, $p = 0.7$]). The number of vesicles per synapse and the number of docked vesicles per synapse were not statistically different between these three conditions (Figure 2B),

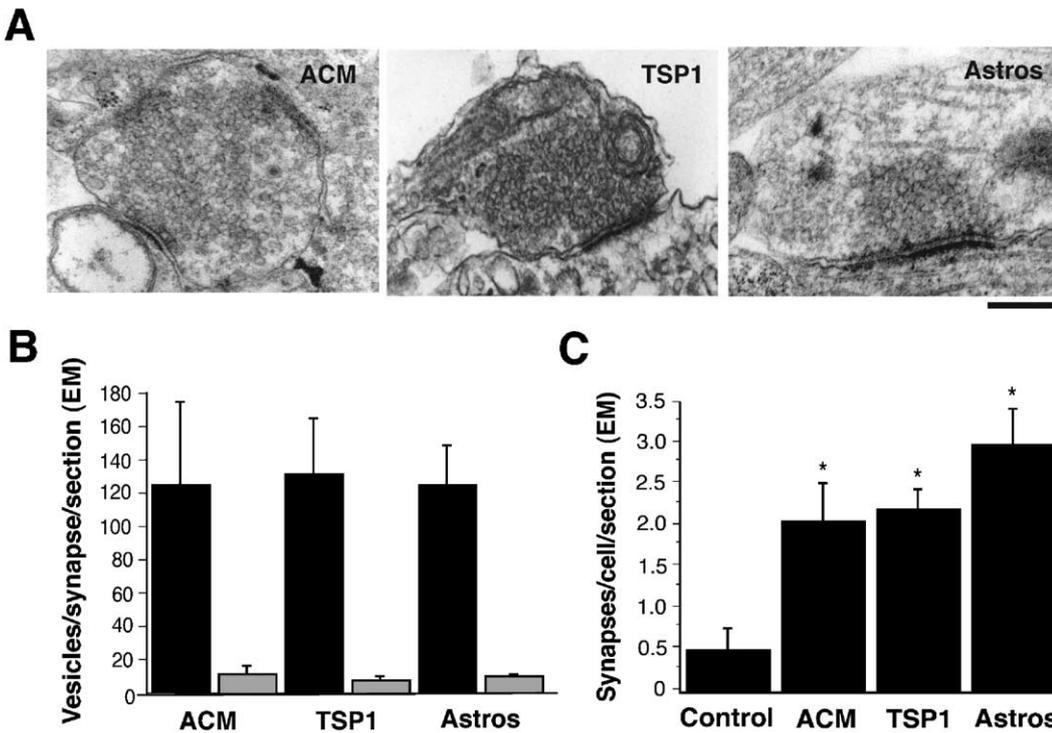


Figure 2. TSP1 Induces Ultrastructurally Normal Synapses

(A) Electron micrographs (EM) of synapses in the presence of ACM, TSP1, or astrocyte feeding layer (Astros). In all cases, ultrastructurally normal synapses are seen.

(B) Quantification of total number of vesicles (black bars) and number of docked vesicles (gray bars) per synapse per section indicates no difference between synapses formed in the presence of ACM, TSP1, or astrocytes, indicating that all three promote formation of normal and indistinguishable ultrastructural synapses.

(C) Quantification of the number of synapses per cell per section measured by EM shows a significant increase in the number of synapses on neurons cultured with ACM, TSP1, or astrocytes compared to control. Asterisks correspond to $p < 0.05$ compared to control. Error bars are the mean \pm SEM. Scale bar is 500 nm.

and the increase in synapse number in all cases was comparable to our immunostaining results (Figure 2C). These findings demonstrate that TSP1 is sufficient to induce ultrastructurally normal synapses and provide evidence that the synaptic structures we detect by immunostaining likely correspond to the fully developed synaptic structures we observe by EM.

TSP2 Is a Necessary Component of the Synapse-Promoting Activity of ACM

Which TSPs are expressed by cultured astrocytes? Of the five members of the TSP family, TSP1 and -2 are highly related and share common functional domains, while TSP -3, -4, and -5/COMP lack some of the domains present in TSP1/2 (Adams, 2001). RT-PCR analysis of mRNA isolated from astrocytes in culture indicated expression of both TSP1 and TSP2 (data not shown). However, we were only able to detect protein for TSP2 by Western blotting of ACM and astrocyte cell lysate with TSP1- and TSP2-specific antibodies (data not shown and Figure 3C), even though the TSP1 antibody recognizes rat TSP1 in serum (data not shown) and rat brain lysate (Figure 5E).

Is TSP2 synaptogenic? We found that recombinant TSP2 (rTSP2) increased synapse number in RGCs to a similar degree as TSP1 (Figures 3A and 3B). This finding

indicates that TSP1 and TSP2 both promote synaptogenesis. In addition, the synaptogenic activity of recombinant TSP2 provides evidence that the activity in purified platelet TSP1 is not due to copurification of a TSP binding protein. This conclusion is further supported by the lack of visible contaminating proteins in the recombinant TSP2 used for these experiments when analyzed by Coomassie staining.

Is TSP2 a necessary component of the ACM activity? When we treated RGCs with ACM and TSP1 together, the increase in synapse number was not larger than that observed with treatment by either alone (Figure 1E), suggesting that ACM and TSP1 share a common pathway. To test directly whether TSP2 is necessary, we immunodepleted TSP2 from ACM with a TSP2-specific antibody (Figure 3C). RGCs cultured in TSP2-depleted ACM developed several-fold fewer synaptic puncta compared to nondepleted ACM, reducing the number of synapses induced to control levels (Figure 3D). Interestingly, despite the lack of double-labeled synaptic puncta in RGCs cultured with TSP2-depleted ACM, there was still a significant increase in the number of single-labeled puncta containing nonoverlapping synaptotagmin or PSD-95 immunoreactivity (Figure 3E). These findings demonstrate that TSP2 is necessary for astrocytes to enhance synaptogenesis and suggest that TSP2 may normally enhance synaptogenesis by inducing

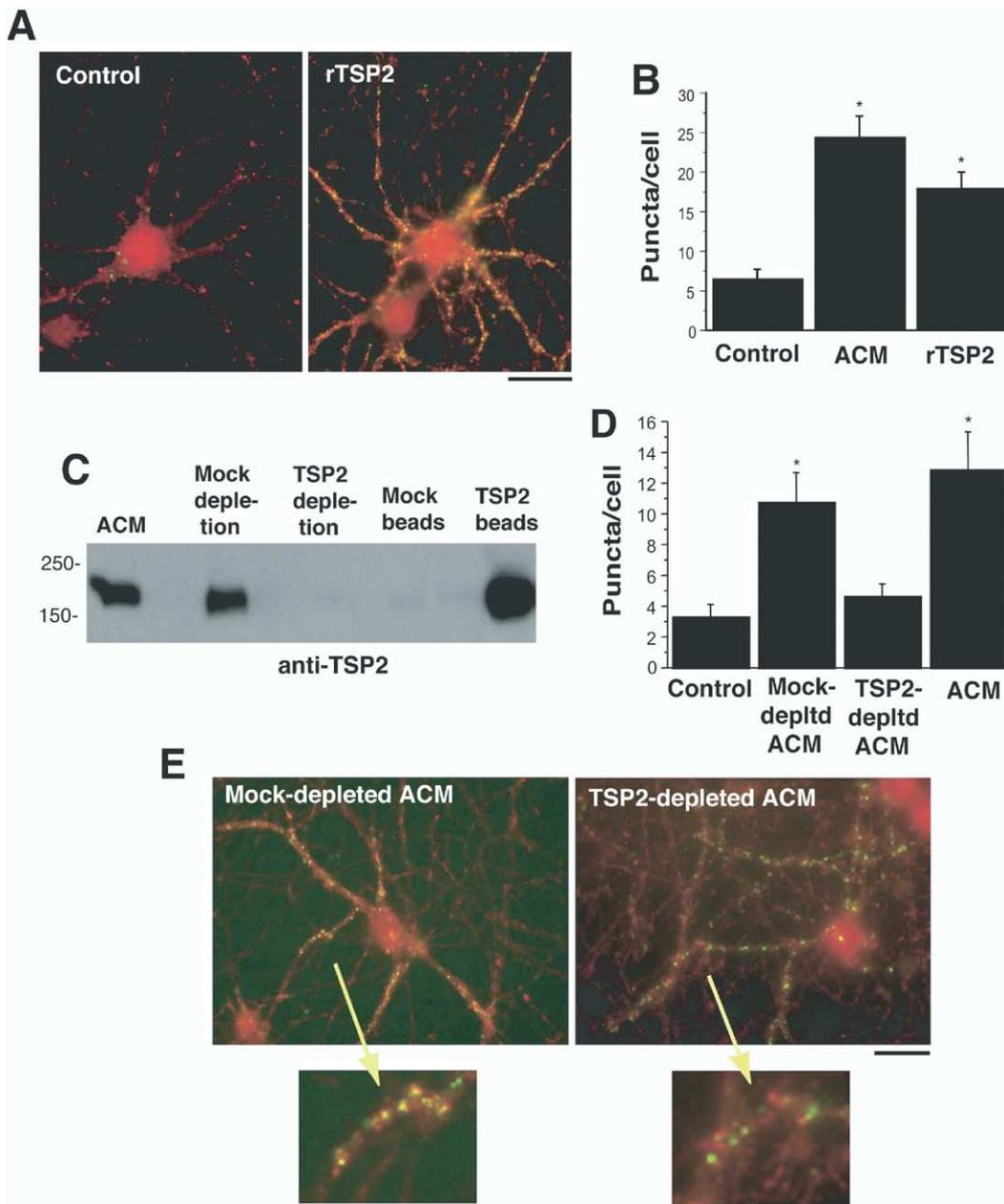


Figure 3. TSP2 Is Necessary for the Increase in Synapse Number Induced by ACM

(A) Immunostaining of RGCs for colocalization of presynaptic synaptotagmin (red) and postsynaptic PSD-95 (green) shows few synaptic puncta in the absence of astrocytes (Control) but many in the presence of recombinant TSP2 (rTSP2).

(B) Quantification of the increase in synaptic puncta with rTSP2 indicates that rTSP2 is sufficient to increase the number of structural synapses. Asterisks correspond to $p < 0.001$ compared to control.

(C) Immunodepletion with a TSP2-specific antibody depletes from ACM.

(D) Depletion of TSP2 from ACM reduces synapse-promoting activity to control levels. Asterisks correspond to $p < 0.05$ compared to control.

(E) Mock-depleted ACM retains full synapse-promoting activity (synaptotagmin, red; PSD-95, green), while TSP2-depleted ACM is depleted of synapse-promoting activity. TSP2-depleted ACM promotes an increase in the number of pre- and postsynaptic labeling on neurons, but the puncta are no longer colocalized. Error bars are the mean \pm SEM. Scale bars are 30 μm .

or maintaining the alignment and/or adherence of pre- and postsynaptic specializations.

ACM and TSP1 Induce Formation of Postsynaptically Silent Synapses

Despite their potent effects on increasing structural synapse number, neither ACM, TSP1, nor TSP2

increased synaptic activity as measured by whole-cell patch clamp recording (Figure 4A; Supplemental Figure S4). In contrast, astrocyte feeding layers significantly increased the frequency of synaptic events (Figure 4A). We next investigated whether the TSP1- and ACM-induced synapses were presynaptically active by measuring vesicular release using an antibody to the

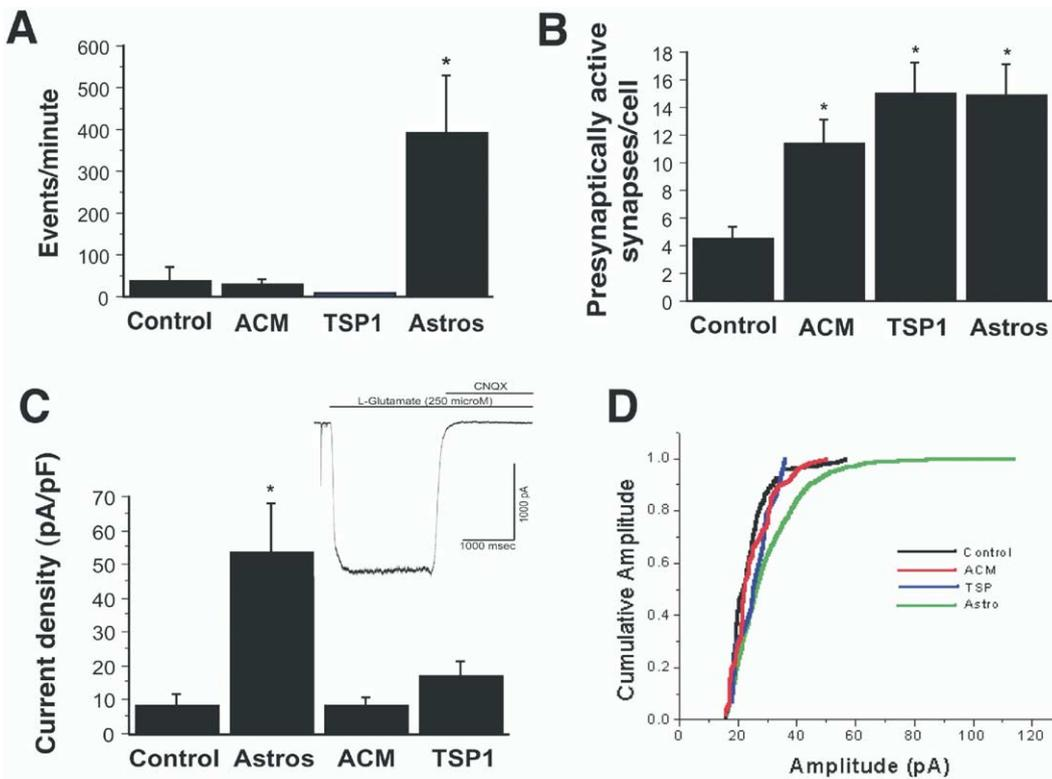


Figure 4. TSP1-Induced Synapses Are Presynaptically Active but Postsynaptically Silent

(A) Measurement of spontaneous mEPSCs shows that neither ACM nor TSP1 increase event frequency above control levels, in contrast to a feeding layer of astrocytes (Astros). (B) RGCs treated with ACM, TSP1, and astrocyte feeding layer (Astros) all have significantly more presynaptic uptake of an anti-synaptotagmin luminal domain antibody than neurons cultured alone (Control), indicating that ACM- and TSP1-induced synapses are presynaptically active. (C) Whole-cell L-glutamate responses indicate that ACM and TSP1 do not increase postsynaptic responses to glutamate above control levels, in contrast to astrocyte feeding layers (Astros). Inset depicts the postsynaptic glutamate response in an RGC grown with an astrocyte feeding layer, indicating that it is mediated by non-NMDA receptors. (D) Measurement of cumulative amplitude distributions reveals that neither ACM nor TSP1 increase mEPSC amplitudes above control, in contrast to astrocyte feeding layer. This indicates that few functional glutamate receptors are present at synaptic sites. These results indicate that TSP1 and ACM do not increase postsynaptic glutamate receptor expression or function. Asterisks in all panels correspond to $p < 0.05$ compared to control. Error bars are the mean \pm SEM.

luminal domain of the vesicular protein synaptotagmin and the styryl dye FM2-10, both of which are taken up in an activity-dependent manner when synaptic vesicles recycle (Kraszewski et al., 1995). Double immunolabeling indicates that most presynaptic puncta overlapped with PSD-95 postsynaptic puncta in all conditions. TSP1, ACM, and an astrocyte feeding layer all increased the number of sites of spontaneous synaptic vesicular recycling in RGCs to a similar extent (Figure 4B; Supplemental Figure S5). This was not due to a general increase in synaptic proteins (Supplemental Figure S2; Ullian et al., 2001). In addition, the fold increase in the number of presynaptically active puncta per cell in all three conditions was similar to the fold increase in the number of structural synapses measured by immunostaining and EM, consistent with the sites of vesicular recycling corresponding to synaptic sites. These results indicate that the majority of synapses induced by astrocyte feeding layers, ACM, and TSP1 are presynaptically active.

To assess postsynaptic function, we first examined whole-cell responses of RGCs cultured in the presence

of TSP1 or ACM to applied glutamate and found that responses were not increased above control levels (Figure 4C). To specifically look at synaptic receptors, we measured the amplitudes of spontaneous miniature events (mEPSCs). The cumulative mEPSC amplitude distribution shows that the synaptic events recorded in RGCs cultured with either TSP1 or ACM are smaller than those induced by a feeding layer of astrocytes and are about 5-fold less sensitive to glutamate (Figure 4D). This suggests that there is a second signal generated in the presence of astrocyte feeding layers that functions by either recruiting glutamate receptors to the synapse or by activating them.

Despite the lack of functional AMPA receptors at ACM- and TSP1-induced synapses, TSP1-induced synapses exhibited normal postsynaptic densities by EM that are strongly immunoreactive for the postsynaptic proteins PSD-95, SAP-102, and Homer (Supplemental Figure S6). Thus, whereas astrocyte-induced synapses are fully functional, both ACM- and TSP1-induced synapses are presynaptically active but are postsynaptically silent, containing fewer functional AMPARs. These

similar properties of ACM- and TSP1-induced synapses provide further evidence that TSPs are a component of the synaptogenic activity of ACM.

RGC synaptic responses *in vitro* and *in vivo* are largely AMPA receptor mediated, with a small NMDA receptor-mediated component in the absence of Mg^{2+} (Chen and Diamond, 2002; Ullian et al., 2004a). In order to determine whether TSP1-induced synapses release glutamate that can activate postsynaptic NMDA receptors, we analyzed the evoked responses of RGCs treated with TSP1 or astrocyte feeding layers in the presence and absence of Mg^{2+} . In contrast to astrocyte feeding layer-induced synapses, RGCs treated with TSP1 exhibited no AMPA component to the evoked response when currents were elicited in the presence of Mg^{2+} , but a small NMDA component was detectable in the absence of Mg^{2+} (Supplemental Figure S4). Thus, despite the lack of postsynaptic AMPA receptors, the TSP-induced synapses are functional in that they release glutamate and exhibit small NMDAR-mediated components of the evoked response.

TSPs Colocalize with Synaptic Markers and Are Expressed by Astrocytes *In Vivo*

To determine whether TSP1 and TSP2 are expressed in the developing brain, we used antiserum against TSP1 to immunostain postnatal brain, the age at which the bulk of synaptogenesis occurs. It is not clear whether this antiserum also recognizes the highly related isoform TSP2, so we refer to the immunoreactivity as TSP1/2. TSP1/2 immunoreactivity was observed throughout the postnatal day 8 (P8) cortex, superior colliculus, and retina, and appears diffuse and widespread, as expected for a matrix molecule secreted by astrocytes (Figure 5 and data not shown). Interestingly, TSP1/2 immunoreactivity was also seen in discrete puncta that colocalized with the synaptic marker synaptotagmin in both cortex (Figure 5A) and superior colliculus (Figure 5B). We also found extensive colocalization of TSP1/2 with ezrin (Figure 5C), a marker of the fine astrocyte processes that ensheath synapses in the postnatal CNS (Derouiche and Frotscher, 2001). Interestingly, TSP1/2 immunoreactivity largely disappeared in these brain regions by postnatal day 21 (P21; Figure 5D), suggesting that TSP1 and TSP2 serve a transient function and are not required for maintenance of synapses in the adult.

In order to more directly determine whether TSP1 and TSP2 proteins are present in the postnatal and adult rat brain, we used TSP1- and TSP2-specific antibodies, which work well for Western blotting but not immunostaining, to look at protein expression. Both TSP1 and TSP2 proteins were detected in extracts prepared from rat P5 cortex (Figure 5E) and whole brain (data not shown). As we observed for the immunoreactivity, both TSP1 and TSP2 protein levels were very low or absent in adult brain. To further examine which TSPs are present in astrocytes in postnatal brain, we performed RT-PCR on mRNA isolated from highly purified, acutely isolated astrocytes from P5 rat cortex. Both TSP1 and TSP2 mRNAs were detected (data not shown). Taken together, these results show that both TSP1 and TSP2 are present in the developing brain, where they are highly localized to astrocytes, and are downregulated in adult brain.

Developing Brains Deficient in TSP1 and TSP2 Form Fewer Synapses

In order to determine if TSP1 and TSP2 play a role in CNS synapse formation *in vivo*, we examined synapse number in brain cryosections prepared from wild-type (wt) mice and mice lacking TSP1, TSP2, or both (Agah et al., 2002) by immunostaining with antibodies to synaptic markers followed by confocal imaging (Figure 6A). No decrease in synapse number was detected in TSP1- or TSP2-deficient mice. However, in the TSP1/2 double null cerebral cortex, there was a 40% decrease in synaptic puncta at P8 as quantified by SV2 immunoreactivity (Figure 6B). Even by P21, a time when synapse number has normally plateaued, there was still a 25% decrease in synaptic puncta compared to wt controls (Figure 6C). A similar decrease in synapse number was observed in TSP1/2 double null brain sections from the superior colliculus (data not shown). There was substantial variability between brain regions and mice, with decreases in cortical synapse number that ranged as high as 50% in some cases. Similar results were obtained using antibodies to other synaptic proteins including Bassoon and PSD-95, indicating that the decreased puncta likely corresponded to a decrease in synapse number rather than simply a decrease in the synaptic localization of a particular protein.

To verify that these puncta correspond to synapses as defined by colocalization of pre- and postsynaptic proteins, we double labeled cryosections of P21 wt and TSP1/2 double null brains using antibodies to the presynaptic protein Bassoon (BSN) and the postsynaptic protein SAP-102 (Lim et al., 2002; Figure 7A). We used novel trichloroacetic acid fixation conditions that allowed both pre- and postsynaptic markers to be simultaneously immunostained. We saw a similar 31% decrease in the number of colocalized pre- and postsynaptic puncta in TSP1/2-deficient brains compared to wt (Figure 7B). Similar to our cell culture results, we did not see an overall decrease in the levels of synaptic proteins in TSP1/2 double null brains compared to wt (Supplemental Figure S7).

To determine whether the effect of TSP1/2 deficiency on synapse number was direct and not secondary to effects on cell survival, proliferation, or migration, we counted the number of DAPI-stained nuclei per section in P21 cortex. We found no significant difference in the number of DAPI nuclei between wt and TSP1/2 double null brains ($85 \pm$ ten nuclei per area wt; $97 \pm$ ten nuclei per area TSP1/2 double null, $p = 0.4$). In addition, there was no obvious difference in the morphology of cortical structures or layers. To determine whether the effect of deleting TSP1/2 on synapse number was due to defects in dendritic arborization, we quantified the density of dendritic fields in synaptic areas of the cortex. We found no significant morphological difference in dendritic structures or dendritic arbor density between wt and TSP1/2 double null brains at P21 or P8 (Figures 7C and 7D). These data, together with the persistent decrease in synapse number at the nearly adult age of P21, provide evidence that the decrease in synapse number in TSP1/2-deficient mice cannot be explained by a decrease in cell number or dendritic number or length but rather is due to a specific inability to form or maintain a normal number of synapses. Taken together,

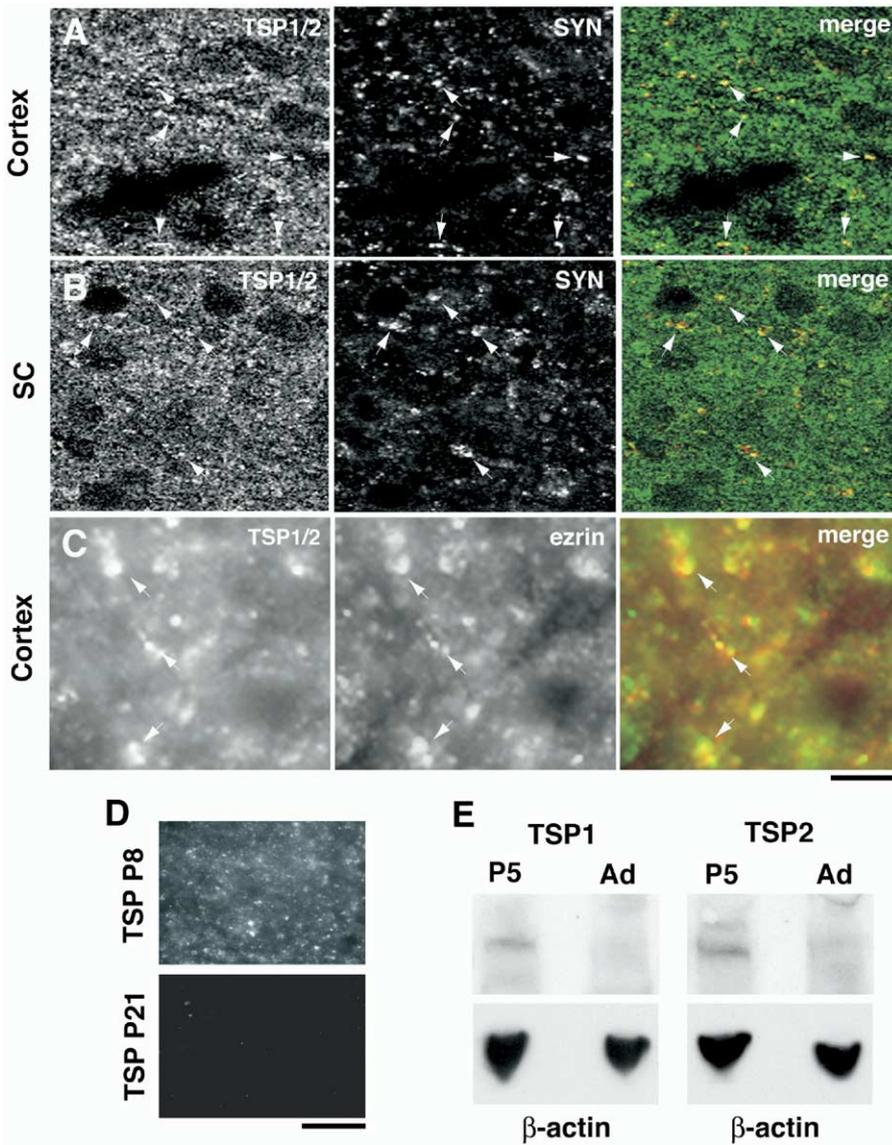


Figure 5. TSP1/2 Immunoreactivity Is Localized to Astrocyte Processes at Many Synapses throughout the Developing Brain
 (A and B) Confocal images of immunolabeled rat P8 brain sections reveal TSP1/2 throughout the cortex and superior colliculus (SC). TSP1/2 immunoreactivity is located at synaptic sites as indicated by double labeling for TSP1/2 and synaptotagmin (SYN).
 (C) Immunolabeling of cortex for TSP1/2 and the fine glial process marker ezrin. Merged images indicate that TSP1/2 is located to fine astrocyte processes, many of which surround synapses.
 (D) Immunostaining of TSP1/2 in P8 and P21 cortex. TSP1/2 immunoreactivity is undetectable by P21.
 (E) Western blot analysis of P5 rat cortical lysates shows that both TSP1 and TSP2 proteins are present in postnatal cortex and are downregulated in adult cortex. Scale bars are 10 μ m (A and B), 2 μ m (C), and 100 μ m (D).

these findings provide evidence that TSP1 and TSP2 are astrocyte-derived proteins that help to promote CNS synaptogenesis in vitro and in vivo.

Discussion

TSP1 and TSP2 Are Astrocyte-Secreted Proteins that Promote CNS Synaptogenesis

The results reported here support several conclusions. First, we show that nonneuronal proteins exist that can

trigger CNS synaptogenesis and identify TSP1 and TSP2 as astrocyte-secreted proteins that are sufficient to induce the formation of ultrastructurally normal CNS synapses. Second, although TSPs induce postsynaptic differentiation as indicated by EM analysis and induction of postsynaptic protein clustering, we find that TSP1- and TSP2-induced synapses are presynaptically active but postsynaptically silent, lacking AMPAR responsiveness. Therefore, an unidentified astrocyte-derived signal is necessary for full postsynaptic func-

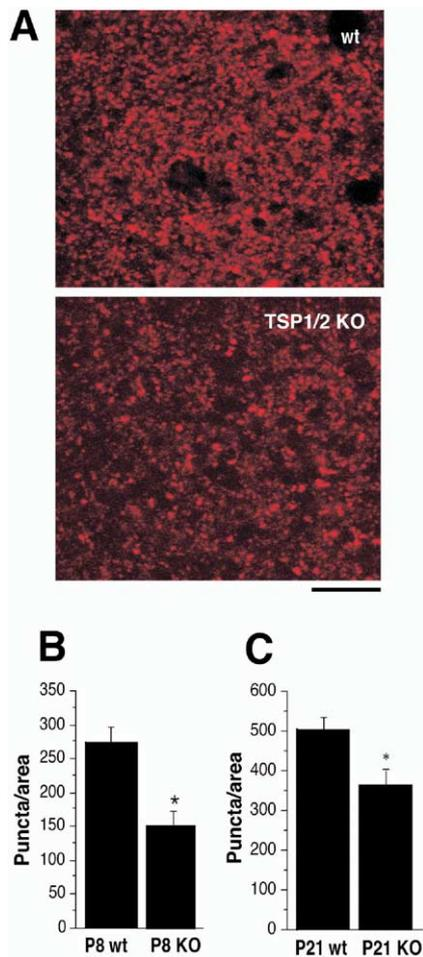


Figure 6. Quantification of Synapse Number in TSP1/2 Double Null Brain

(A) Confocal sections of P21 rat cortex immunostained for presynaptic marker SV2 in wt and TSP1/2 double null brains. Scale bar is 10 μ m.

(B) Quantification of synaptic puncta in matched cortical fields from P8 wt and TSP1/2 double null brains. A significant reduction in synapse number in TSP1/2 double null brains was found ($p = 0.0046$).

(C) Quantification of synaptic puncta in matched cortical fields from P21 wt and TSP1/2 double null brain. A significant reduction in synapse number in TSP1/2 double null brains was found ($p = 0.0169$). Error bars are the mean \pm SEM.

tion in vitro. Third, TSP2 is necessary for the ability of astrocytes to induce the formation of structural synapses between RGCs in vitro. Fourth, TSP1 and TSP2 are expressed in the postnatal but not adult CNS where they are broadly localized in astrocytes and synapses, as expected for an astrocyte-secreted matrix molecule. Finally, mice lacking both TSP1 and TSP2 have a substantially reduced number of synapses in many CNS regions, indicating that these TSPs help to promote normal CNS synaptogenesis in vivo. It is possible that the degree of synapse loss might be substantially larger in the absence of additional TSP family members, given that both TSP3 and TSP4 may be expressed in adult brain (Arber and Caroni, 1995; Iruela-Arispe et al., 1993).

TSP-Induced Synapses Are Postsynaptically Silent

An important implication from this study is that astrocyte-induced CNS synapse formation in culture requires at least two steps that are mechanistically distinct. First, TSPs induce the formation of ultrastructurally normal synapses bearing pre- and postsynaptic specializations that are presynaptically active but postsynaptically silent. Second, an unidentified astrocyte signal induces postsynaptic function by inserting functional AMPARs into postsynaptic sites. In preliminary experiments, we have found that feeding layers of astrocytes but not ACM or TSP induce clustered AMPA receptor immunoreactivity at postsynaptic sites on RGCs. This is reminiscent of the two-step model for activation of silent synapses in the developing brain thought to be important for synapse refinement and circuit modification wherein silent structural synapses are initially formed and some become postsynaptically functional in a second step involving an activity-dependent LTP mechanism (Isaac et al., 1997; Malenka and Nicoll, 1997). Our findings provide evidence that astrocytes may be actively involved in both of these steps.

How Do TSPs Induce Synaptogenesis?

Many neuronal molecules work in concert to build a CNS synapse. The transmembrane neuronal proteins neuroligin and neuexin constitute an important part of the intrinsic synaptic machinery (reviewed in Scheiffele [2003]; Chih et al. [2005]; Graf et al. [2004]). They work in concert with a number of soluble neuronal proteins that specifically promote either post- or presynaptic differentiation including ephrins, Narp/NP2, Wnt7A, and FGF22 (Scheiffele, 2003; Umemori et al., 2004), as well as with soluble astrocyte-derived signals such as cholesterol (Mauch et al., 2001) and an as yet unidentified signal reported here, that further help to promote pre- and postsynaptic function. We have shown that TSP1 and TSP2 are necessary and sufficient to induce synapses that exhibit both pre- and postsynaptic differentiation.

How do TSP1 and TSP2 induce synaptogenesis? The increase in synapse number by TSPs could be caused by an increase in formation of new synapses, stabilization of existing synapses, or both. Because RGC synapses are rapidly lost when astrocytes are removed, the simplest possibility is that TSPs act by stabilization. In the developing brain, initially formed synapses might be immature and highly plastic, with TSPs serving to increase synapse number by locking synapses into place. The well-known ability of TSPs to regulate cell adhesion fits well with this possibility. In addition, RGCs cultured in TSP2-depleted ACM failed to form synapses but exhibited a large number of pre- and postsynaptic specializations that were not juxtaposed. This could be a result of initial synapse formation followed by destabilization and is reminiscent of the misalignment phenotype that occurs at the neuromuscular junction in the absence of laminin α 4, where synaptic specializations are present but not precisely apposed (Patton et al., 2001).

We do not know yet whether TSPs act at the cell body or at axon terminals. However, the several day

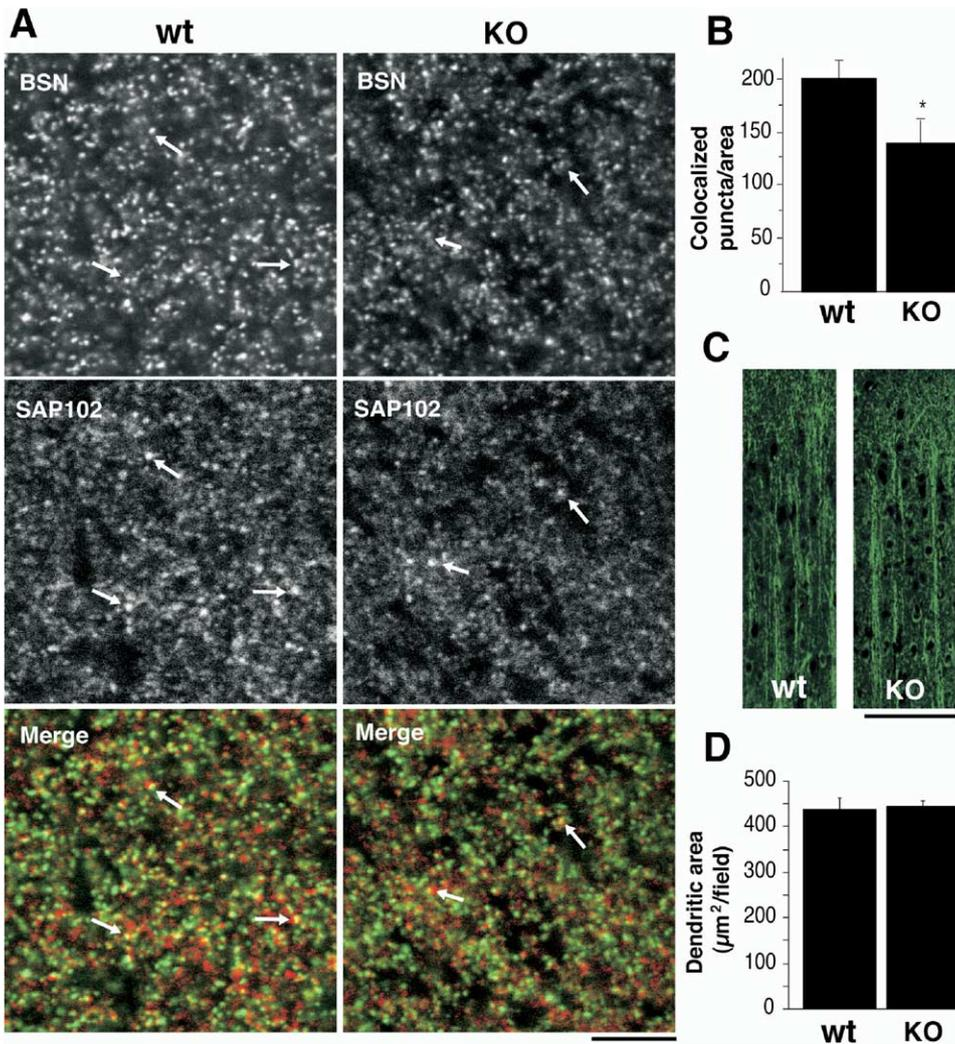


Figure 7. Quantification of Colocalization of Pre- and Postsynaptic Puncta in TSP1/2 Double Null Brain

(A) Wt and TSP1/2 double null P21 cortex immunolabeled for presynaptic Bassoon (BSN) and postsynaptic SAP102. Fewer synaptic puncta containing both pre- and postsynaptic markers are present in TSP1/2 double null brains compared to wt. Scale bar is 6 μm .

(B) Quantification of colocalization of pre- and postsynaptic markers in brain sections from wt and TSP1/2 P21 double null brains. A 31% reduction in the number of colocalized synaptic puncta was observed in TSP1/2 double null brains compared to wt brains ($p = 0.026$).

(C) MAP2 immunostaining in P21 wt and TSP1/2 double null brain. Scale bar is 120 μm .

(D) Quantification of dendritic area shows no difference in dendritic fields ($p > 0.05$). Error bars are the mean \pm SEM.

period required to see the effect of TSPs strongly suggests the possibility that they may act at least in part by inducing neurons to alter expression of proteins that participate in synaptogenesis. A number of known TSP receptors are concentrated at CNS synapses, including RGC synapses (C. Eroglu and B.A.B., unpublished data). Known TSP receptors include the CD47 integrin-associated protein (CD47/IAP), a variety of integrins, and the low-density lipoprotein receptor-related protein LRP1. By binding to one or more of these receptors, TSPs might activate downstream pre- and/or postsynaptic signaling cascades that induce the formation of synaptic adhesions. Alternatively or in addition, TSPs are capable of functioning as adhesive proteins under certain circumstances (Murphy-Ullrich, 2001) and thus might switch growth cones from a neurite out-

growth mode into a synaptogenic mode by allowing them to adhere to outgrowth promoting substrates. Identification of the relevant TSP receptor should help to distinguish between these possibilities.

An important question for future research will be to determine whether TSP promotes synapse formation by acting instructively or permissively. An instructive model would imply that local concentrations of TSPs at particular synapses help determine which synapses are formed and which are not; a permissive model would imply that the presence of TSP is necessary for synapse formation or maintenance but that other signaling events control exactly which synapses are formed. The broad distribution of TSP1/2 localization, the possibility that it acts transcriptionally, and its specific window of developmental timing favor a permissive model.

Implications of CNS Synaptogenic Proteins for Understanding Normal CNS Development and Disease

The identification of TSP1 and TSP2 as CNS synaptogenic proteins has important implications. The abundance of TSPs *in vivo* is dynamically regulated during development, being low in late embryonic brain, higher in postnatal brain, and low or absent in the adult brain (Iruela-Arispe et al., 1993). The CNS levels of TSP1 and TSP2 thus correlate closely with the time interval when the rodent brain normally forms synapses during the first 3 postnatal weeks, and release of astrocyte-derived TSPs could explain the close temporal and spatial correlation of astrocyte development with synapse development (Ullian et al., 2001). Moreover, the downregulation of TSP1/2 levels in adult brain correlates with the relatively poor ability of the adult CNS to form new synapses. These results therefore suggest the hypothesis that TSP1/2 levels act as a permissive switch that helps to control the timing of CNS synaptogenesis and raise the question of whether administration of exogenous TSP1/2 would restore the synaptogenic capacity of normal adult brain or enhance the regeneration of new synapses in injured adult brain.

Although TSP1 and TSP2 levels are normally low in the adult brain, reactive astrocytes and activated microglia express these proteins (Lin et al., 2003; Moller et al., 1996). Reemergence of TSPs in reactive astrocytes could thus help to explain the formation of unwanted, extra synapses that result in epilepsy at astrocytic scars as well as help to explain the tendency of axotomized axons to synaptically differentiate and fail to regenerate when they contact reactive astrocytes (Liu et al., 1987). If so, drugs that agonize or antagonize TSPs may help to promote synaptic plasticity and repair in many CNS diseases.

In conclusion, we have shown that TSPs are astrocyte-derived proteins that help to promote CNS synaptogenesis and that they work in concert with other, as yet unidentified, astrocyte-derived signals to produce functional synapses. Our findings, together with other recent work (reviewed in Ullian et al. [2004b]), increasingly suggest that astrocytes should no longer be viewed primarily as passive support cells but rather as cells that actively help to control the formation and function of synapses in developing and adult organisms.

Experimental Procedures

Purification and Culture of RGCs

Step-by-step protocols for all procedures are available on request to barres@stanford.edu. RGCs were purified by sequential immunopanning to greater than 99.5% purity from P5 Sprague-Dawley rats (Simonsen Labs, Gilroy, CA) and cultured in serum-free medium containing BDNF, CNTF, and forskolin on laminin-coated coverslips, as previously described (Barres et al., 1988; Meyer-Franke et al., 1995; Ullian et al., 2001).

Purified human platelet TSP1 was obtained from either Sigma or Haematologic Technologies. Recombinant TSP2 was purified from serum-free medium conditioned by baculovirus-infected insect cells expressing mouse TSP2. Since purified TSP1 is readily available, we used this as the source of TSP in our experiments unless otherwise noted. TSPs were used at a concentration of 5 μ g/ml

(\sim 10 nM). Biglycan, CSPG A, CSPG C, decorin, and osteopontin were from Sigma; agrin was from R&D Systems; collagen IV was from BD Biosciences; fibronectin, osteonectin, and vitronectin were from Haemtech; and tenascin C was a generous gift from M. Schachner. All matrix molecules were used at a concentration of 5 μ g/ml, except collagen IV, which was used at 10 μ g/ml, and the CSPGs, which were used at 1 μ g/ml to avoid overfasciculation. GDNF (10 ng/ml), TNF α (10 ng/ml), TGF β 1 (10 ng/ml), bFGF (10 ng/ml), and HGF (50 ng/ml) were from Preprotech; IL-6 (10 ng/ml) was from Sigma; and pleiotrophin (50 ng/ml) was from R&D Systems. RGCs were cultured for 3–4 days to allow robust process outgrowth and then cultured with astrocyte feeding layers, ACM or factors for an additional 6 days. TTX and Picrotoxin were obtained from RBI. All other reagents were obtained from Sigma. Cholesterol was used at a final concentration of 10 μ g/ml.

Preparation of Astrocytes and ACM

Cortical astrocytes were prepared as described (McCarthy and de Vellis, 1980). Astrocytes were then plated onto 24-well inserts (Falcon, 1.0 μ m) or 10 cm tissue culture dishes. For preparation of ACM, confluent cultures of astrocytes in 10 cm dishes were washed three times in PBS and fed with 10 ml RGC medium (without CNTF, BDNF, or forskolin). ACM was harvested after 4–6 days of conditioning, filtered through a 0.2 μ m syringe filter, and concentrated ten times through a 5 kDa molecular weight cutoff centrifuge concentrator (Millipore), unless otherwise indicated. ACM was used at a final concentration of 5 \times unless otherwise indicated. RGCs were cultured for 4 days to allow robust process outgrowth and then cultured with ACM or an astrocyte feeding layer for an additional 6 days.

Electrophysiology

Membrane currents were recorded by whole-cell patch clamping at room temperature (18°C–22°C) at a holding potential of -70 mV unless otherwise specified. Patch pipettes (3–10 M Ω) were pulled from borosilicate capillary glass (WPI). For recordings of synaptic or whole-cell glutamate currents, the bath solution contained (in mM) 120 NaCl, 3 CaCl₂, 2 MgCl₂, 5 KCl, and 10 HEPES (pH 7.3). For recording in Mg²⁺-free conditions, the external bath solution contained (in mM) 140 NaCl, 3.5 KCl, 10 HEPES, 20 glucose, 3 CaCl₂, and 20 μ M glycine (pH 7.3). TTX (2 μ M) and bicuculline (10 μ M) were added for spontaneous miniature event recordings. The internal solution contained (in mM) 100 K-gluconate, 10 KCl, 10 EGTA (Ca²⁺ buffered to 10⁻⁶ molar), and 10 HEPES (pH 7.3). For recordings of autaptic currents, the internal solution contained (in mM) 122.5 K-gluconate, 8 NaCl, 10 HEPES, 0.2 EGTA, 2 Mg-ATP, 0.3 Na-GTP, 20 K₂-creatine phosphate, and phosphocreatine kinase (50 U/ml). Currents were recorded using pClamp software for Windows (Axon Instruments, Foster City, CA). Glutamate (250 mM) and CNQX (10 μ M) were rapidly applied by a quartz microtube array (Superfusion System, ALA Scientific Instruments, New York). Mini excitatory postsynaptic currents (mEPSCs) were analyzed using Mini Analysis Program (SynaptoSoft, Decatur, GA) and plotted using SigmaPlot (SPSS, Chicago, IL) or Origin (Microcal, Northampton, MA).

Synaptic Assays

For synapse quantification, cultures were fixed for 7 min in 4% paraformaldehyde (PFA), washed three times in phosphate-buffered saline (PBS), and blocked in 100 μ l of a blocking buffer containing 0.1% Triton X-100 for 30 min. After blocking, cover slips were washed three times in PBS, and 100 μ l of primary antibody solution was added to each cover slip, consisting of rabbit anti-synaptotagmin (cytosolic domain, Synaptic Systems) and mouse anti-PSD-95 (6G6-1C9 clone, Affinity Bio Reagents) or rabbit anti-GluR2/3 (Chemicon) diluted 1:500 in antibody buffer. Coverslips were incubated overnight at 4°C, washed three times in PBS, and incubated with 100 μ l of Alexa-594 conjugated goat anti-rabbit and Alexa-488 conjugated goat anti-mouse (Molecular Probes) diluted 1:1000 in antibody buffer. Following incubation for 2 hr, coverslips were washed five times in PBS and mounted in Vectashield mounting medium with DAPI (Vector Laboratories Inc) on glass slides

(VWR Scientific). For presynaptic activity assay, rabbit synaptotagmin antiserum was generated by immunization with a peptide corresponding to the N-terminal luminal portion of synaptotagmin. This serum was added at 1:500 to live cultures and incubated for 6 hr. Cells were then washed three times in DPSB, fixed, and stained as above, except for the omission of synaptotagmin antibody from the primary antibody solution. Secondary-only controls were routinely performed and revealed no significant background staining.

Mounted coverslips were imaged using Nikon Diaphot and Eclipse epifluorescence microscopes (Nikon). Conditions were determined positive and warranted further analysis if a difference in colocalized puncta could be detected by eye, an increase of approximately 20%, in both duplicate coverslips. Healthy cells that were at least two cell diameters from their nearest neighbor were identified and selected at random by eye using DAPI fluorescence. Eight bit digital images of the fluorescence emission at both 594 nm and 488 nm were recorded for each selected cell using a cooled monochrome CCD camera and SPOT image capture software (Diagnostic Instruments, Inc). These manipulations were performed automatically using the custom software package SpotRemover (Barry Wark, source code and/or binaries available upon request to bwark@stanford.edu/barrywark@mac.com) on Macintosh OS X.

Colocalized puncta were identified using a custom-written plug-in (Barry Wark, licensed under the GPL [<http://www.gnu.org/copyleft/gpl.html>]) for the NIH image processing package ImageJ v1.24 and greater (available at <http://rsb.info.nih.gov/ij/>). Full documentation of the puncta-counting algorithm is available in the "Puncta Analyzer" plug-in's source code. We verified that this analysis generates counts that are similar to the numbers we obtain counting by eye.

Immunodepletion and Western Analysis

ACM (10 \times) was incubated with 20 μ l goat anti-ApoE (a generous gift from Karl Weisgraber, UCSF) or 10 μ l rabbit anti-TSP2 serum (Tooney et al., 1998) overnight at 4°C. Primary antibodies with bound proteins were removed from ACM by incubation with 20 μ l protein G or protein A-Sepharose beads (Pierce), respectively, for 2 hr at 4°C followed by centrifugation to separate the supernatant, and a sample was saved for Western blotting before addition to RGC cultures.

For preparation of P5 and adult rat or P8 mouse cortical lysates, cortices were homogenized in 20 volumes w/v lysis buffer (25 mM Tris 7.4, 150 mM NaCl, Complete Protease Inhibitor Cocktail [Roche]). After homogenization, sodium deoxycholate was added to a final concentration of 1%, and homogenate was solubilized at 4°C for 30 min with rocking. Lysates were cleared by centrifugation at 16 \times g for 20 min at 4°C, and 30 μ g of each lysate was used for Western analysis. For preparation of RGC lysates, RGCs cultured in 6-well dishes were lysed with M-PER Mammalian Protein Extraction Reagent (Pierce), incubated at 4°C for 30 min, and cleared by centrifugation at 16 \times g for 10 min at 4°C. Each lysate was loaded at 5 μ g per lane.

Proteins in ACM or lysates were resolved by SDS-PAGE and transferred onto PVDF (Millipore). Membranes were incubated in blocking buffer (PBS containing 0.1% Tween-20 and 5% nonfat milk) for 30 min at room temperature, followed by incubation for 1 hr or overnight at 4°C in blocking buffer containing either rabbit anti-ApoE (1:500, a generous gift from Karl Weisgraber, UCSF), mouse anti-TSP1 (1:250, BD Transduction), mouse anti-TSP2 (1:250, BD Transduction), rabbit anti-synaptotagmin (1:1000, Synaptic Systems), mouse anti-PSD-95 (1:000, clone 6G6-1C9, Affinity BioReagents), mouse anti- β -actin (1:2000, AC-15, Sigma), mouse anti-synapsin (1:5000, clone 46.1, Synaptic Systems), rabbit anti-SAP102 (1:1000, J.W.H.), or rabbit anti-Bassoon (1:200, Synaptic Systems). Immunoreactive proteins were detected using HRP-conjugated anti-rabbit or anti-mouse IgG (1:10,000; Jackson Immuno-research) and visualized with a chemiluminescent substrate for HRP (SuperSignal West Pico; Pierce Chemicals). Protein levels were quantified using ImageJ (NIH).

Immunohistochemistry

Brains were immersion fixed in 4% PFA overnight or, for double labels of synaptic puncta, brains were immersion fixed in 10%

trichloroacetic acid for 1 hr at RT (Hayashi et al., 1999). Brains were then washed in 30 mM glycine PBS and sunk in 30% sucrose PBS overnight at 4°C. Brain sections were dried 30 min at 37°C followed by application of blocking buffer. Slides were washed 3 \times 5 min in PBS. Primary antibodies used were diluted into antibody buffer as follows: TSP1 (P10, mouse monoclonal, Immunotech, 1:200 or Ab 8, Neomarkers, rabbit, 1:200), synaptotagmin (rabbit polyclonal, Synaptic Systems, 1:500), ezrin (monoclonal 3C12, Neomarkers, 1:200), SV2 (hybridoma supernatant, Developmental Studies Hybridoma Bank, 1:30), Bassoon (Stressgen, 1:400), PSD-95 (monoclonal 6G6-1C9, Affinity Bioreagents, 1:250), SAP-102 (J.W.H.; 1:200), and incubated overnight at 4°C followed by three washes in PBS. Secondary Alexa-conjugated antibodies (Molecular Probes) were added at 1:1000 for 2 hr at RT. Slides were washed three times in PBS and mounted in Vectashield plus DAPI.

Electron Microscopy

Cells were prepared for EM using glutaraldehyde as previously described (Ullian et al., 2001) and viewed with a Philips Electronic Instruments CM-12 transmission electron microscope. Synapses were counted by eye under the electron microscope by finding a cell body and dendrites and counting all synapses within a circular field of radius approximately one cell body diameter. Docked vesicles were identified as those within 50 nm from the presynaptic density. Postsynaptic density thickness and length were measured by drawing a line along the visible portion of the density thickness or length and automatically measuring line distance using ImageJ.

Confocal Analysis of Synapse Number

Images of immunostained brains were collected on a Leica SPS SP2 AOBS confocal microscope. Optical sections were line averaged and collected at 0.28 μ m intervals. Gain, threshold, and black levels were individually adjusted per section to cover the same range of pixel values or were set for the wt sections and kept constant for all sections. Stacks of 20 optical sections were quantified for synapse number by projecting a series of five optical sections, a number empirically determined to optically section the entirety of most synaptic puncta, and counting the number of synapses in each projection volume. For double-label experiments, single scans were taken of equivalent cortical areas in wt or KO brains. Synapses were automatically counted using the ImageJ puncta analyzer program and the accuracy of the counts confirmed by counting by hand. $n = 6$ hemispheres for P8 wt and KO, and $n = 10$ hemispheres and for P21 wt and KO. On average, three stacks per hemisphere were obtained, yielding a total of 18 stacks (72 optical sections) for synaptic puncta analysis for P8 brains and a total of 30 stacks (120 optical sections) for synaptic puncta analysis for P21 brains. For double-label experiments, three brains from each condition (KO and wt) were sectioned and scanned. A total of 80 scans for wt and 80 scans for KO were done, and the number of colocalized puncta was determined by using ImageJ.

Supplemental Data

Supplemental Data include seven figures, one table, and Supplemental References and can be found with this article online at <http://www.cell.com/cgi/content/full/120/3/421/DC1/>.

Acknowledgments

We thank Dr. Craig Garner (Stanford) for helpful comments on the manuscript. The ApoE antibody used in the depletion studies was a gift from Dr. Karl Weisgraber (UCSF). BDNF and CNTF/Axokine were generously supplied by Regeneron Pharmaceuticals. This work was supported by grants from the National Institute of Drug Addiction (DA15043; B.A.B.), a Zaffaroni Fellowship (E.M.U.), a National Eye Institute NRSA postdoctoral fellowship (EY07033; K.S.C.), the National Institute for Arthritis and Musculoskeletal Diseases (AR45418; P.B.), a Beginning Grant-in-Aid from the American Heart Association (A.A.), and the National Heart, Lung and Blood Institute (HL68003; J.L.). We would like to extend special thanks to Jonathan Pollock for his support and encouragement of the work.

Received: June 10, 2004
Revised: October 13, 2004
Accepted: December 17, 2004
Published: February 10, 2005

References

- Adams, J.C. (2001). Thrombospondins: multifunctional regulators of cell interactions. *Annu. Rev. Cell Dev. Biol.* 17, 25–51.
- Adams, J.C., and Tucker, R.P. (2000). The thrombospondin type 1 repeat (TSR) superfamily. *Dev. Dyn.* 218, 280–299.
- Agah, A., Kyriakides, T.R., Lawler, J., and Bornstein, P. (2002). The lack of thrombospondin-1 (TSP1) dictates the course of wound healing in double-TSP1/TSP2-null mice. *Am. J. Pathol.* 161, 831–839.
- Arber, S., and Caroni, P. (1995). Thrombospondin-4, an extracellular matrix protein expressed in the nervous system, promotes neurite outgrowth. *J. Cell Biol.* 131, 1083–1094.
- Barres, B.A., Silverstein, B.E., Corey, D.P., and Chun, L.L. (1988). Immunological, morphological, and electrophysiological variation among retinal ganglion cells purified by panning. *Neuron* 1, 791–803.
- Bornstein, P. (2001). Thrombospondins as matricellular modulators of cell function. *J. Clin. Invest.* 107, 929–934.
- Chen, S., and Diamond, J.S. (2002). Synaptically released glutamate activates extrasynaptic NMDA receptors on cells in the ganglion cell layer of rat retina. *J. Neurosci.* 22, 2165–2173.
- Chih, B., Engelman, H., and Scheiffle, P. (2005). Control of excitatory and inhibitory synapse formation by neuroligins. *Science*, in press.
- DeFreitas, M.F., Yoshida, C.K., Frazier, W.A., Mendrick, D.L., Kypta, R.M., and Reichardt, L.F. (1995). Identification of integrin alpha 3 beta 1 as a neuronal thrombospondin receptor mediating neurite outgrowth. *Neuron* 15, 333–343.
- Derouiche, A., and Frotscher, M. (2001). Peripheral astrocyte processes: monitoring by selective immunostaining for the actin-binding ERM proteins. *Glia* 36, 330–341.
- Graf, E.R., Zhang, X., Jin, S.X., Linhoff, M.W., and Craig, A.M. (2004). Neurexins induce differentiation of GABA and glutamate postsynaptic specializations via neuroligins. *Cell* 119, 1013–1026.
- Hayashi, K., Yonemura, S., Matsui, T., and Tsukita, S. (1999). Immunofluorescence detection of ezrin/radixin/moesin (ERM) proteins. *J. Cell Sci.* 112, 1149–1158.
- Iruela-Arispe, M.L., Liska, D.J., Sage, E.H., and Bornstein, P. (1993). Differential expression of thrombospondin 1, 2, and 3 during murine development. *Dev. Dyn.* 197, 40–56.
- Isaac, J.T., Crair, M.C., Nicoll, R.A., and Malenka, R.C. (1997). Silent synapses during development of thalamocortical inputs. *Neuron* 18, 269–280.
- Kraszewski, K., Mundigl, O., Daniell, L., Verderio, C., Matteoli, M., and De Camilli, P. (1995). Synaptic vesicle dynamics in living cultured hippocampal neurons. *J. Neurosci.* 15, 4328–4342.
- Lawler, J. (2000). The functions of thrombospondin-1 and -2. *Curr. Opin. Cell Biol.* 12, 634–640.
- Lim, A., Hall, D.D., and Hell, J.W. (2002). Selectivity and promiscuity of the first and second PDZ domains of PSD-95 and synapse-associated protein 102. *J. Biol. Chem.* 277, 21697–21711.
- Lin, T.N., Kim, G.M., Chen, J.J., Cheung, W.M., He, Y.Y., and Hsu, C.Y. (2003). Differential regulation of thrombospondin-1 and thrombospondin-2 after focal cerebral ischemia/reperfusion. *Stroke* 34, 177–186.
- Liuzzi, F.J., and Lasek, R.J. (1987). Astrocytes block axonal regeneration in mammals by activating the physiological stop pathway. *Science* 237, 642–645.
- Malenka, R.C., and Nicoll, R.A. (1997). Silent synapses speak up. *Neuron* 19, 473–476.
- Mauch, D.H., Nagler, K., Schumacher, S., Goritz, C., Muller, E.C., Otto, A., and Pfrieger, F.W. (2001). CNS synaptogenesis promoted by glia-derived cholesterol. *Science* 294, 1354–1357.
- McCarthy, K.D., and de Vellis, J. (1980). Preparation of separate astroglial and oligodendroglial cell cultures from rat cerebral tissue. *J. Cell Biol.* 85, 890–902.
- Meyer-Franke, A., Kaplan, M.R., Pfrieger, F.W., and Barres, B.A. (1995). Characterization of the signaling interactions that promote the survival and growth of developing retinal ganglion cells in culture. *Neuron* 4, 805–819.
- Moller, J.C., Klein, M.A., Haas, S., Jones, L.L., Kreutzberg, G.W., and Raivich, G. (1996). Regulation of thrombospondin in the regenerating mouse facial motor nucleus. *Glia* 17, 121–132.
- Murphy-Ullrich, J.E. (2001). The de-adhesive activity of matricellular proteins: is intermediate cell adhesion an adaptive state? *J. Clin. Invest.* 107, 785–790.
- Nagler, K., Mauch, D.H., and Pfrieger, F.W. (2001). Glia-derived signals induce synapse formation in neurones of the rat central nervous system. *J. Physiol.* 533, 665–679.
- Neugebauer, K.M., Emmett, C.J., Venstrom, K.A., and Reichardt, L.F. (1991). Vitronectin and thrombospondin promote retinal neurite outgrowth: developmental regulation and role of integrins. *Neuron* 6, 345–358.
- Patton, B.L., Cunningham, J.M., Thyboll, J., Kortessmaa, J., Westerbald, H., Edstrom, L., Tryggvason, K., and Sanes, J.R. (2001). Properly formed but improperly localized synaptic specializations in the absence of laminin alpha4. *Nat. Neurosci.* 4, 597–604.
- Pfrieger, F.W., and Barres, B.A. (1997). Synaptic efficacy enhanced by glial cells in vitro. *Science* 277, 1684–1687.
- Scheiffle, P. (2003). Cell-cell signaling during synapse formation in the CNS. *Annu. Rev. Neurosci.* 26, 485–508.
- Scott-Drew, S., and French-Constant, C. (1997). Expression and function of thrombospondin-1 in myelinating glial cells of the central nervous system. *J. Neurosci. Res.* 50, 202–214.
- Tooney, P.A., Sakai, T., Sakai, K., Aeschlimann, D., and Mosher, D.F. (1998). Restricted localization of thrombospondin-2 protein during mouse embryogenesis: a comparison to thrombospondin-1. *Matrix Biol.* 17, 131–143.
- Ullian, E.M., Sapperstein, S.K., Christopherson, K.S., and Barres, B.A. (2001). Control of synapse number by glia. *Science* 291, 657–661.
- Ullian, E.M., Barkis, W.B., Chen, S., Diamond, J.S., and Barres, B.A. (2004a). Invulnerability of retinal ganglion cells to NMDA excitotoxicity. *Mol. Cell. Neurosci.* 26, 544–557.
- Ullian, E.M., Christopherson, K.S., and Barres, B.A. (2004b). Role for glia in synaptogenesis. *Glia* 47, 209–216.
- Ullian, E.M., Harris, B.T., Wu, A., Chan, J.R., and Barres, B.A. (2004c). Schwann cells and astrocytes induce synapse formation by spinal motor neurons in culture. *Mol. Cell. Neurosci.* 25, 241–251.
- Umehara, H., Linhoff, M.W., Ornitz, D.M., and Sanes, J.R. (2004). FGF22 and its close relatives are presynaptic organizing molecules in the mammalian brain. *Cell* 118, 257–270.